Chapter 3

Potassium currents in neuronal-like cell lines, models to study non-genomic Mineralocorticoid Receptor functionality

Femke L. Groeneweg[1], Henk Karst[2],
Roel de Rijk[1], E. Ron de Kloet[1], Marian Joëls[2]

[1] Department of Medical Pharmacology, Leiden University / LUMC, Leiden, The Netherlands.
[2] Department of Neuroscience and Pharmacology, University Medical Center Utrecht, Utrecht, The Netherlands.

Many rapid non-genomic actions of corticosterone in the brain act through the membrane-associated subpopulation of the MR, including a rapid reduction in fast-inactivated A-type potassium currents by corticosterone. Here we present two attempts to reproduce this membrane-associated role of the MR in neuronal-like cell lines. In differentiated NS-1 cells we obtain A-type potassium currents. Corticosterone did not affect these currents in empty-vector transfected cells. Importantly, upon transfection with the MR both corticosterone and cort-BSA did lead to a rapid reduction of A-type current amplitude ($> 25\,\%$). In contrast, the slowly-inactivated potassium currents in N1E-115 cells were not affected by corticosterone in the presence of the MR. The MR is thus sufficient for a rapid inhibition of fast-inactivated potassium channels by corticosterone and this effect is specific for certain subtypes of potassium channels. We further find that the MR is very instable in an *in vitro* setting and that successful DNA transfection and MR mRNA transcription does not necessarily lead to detectable MR protein levels.

3.1 Introduction

Corticosteroids play a major role in the response of the brain to stress. Within the brain, corticosteroids exert their actions through two receptors: the GR and MR. For many years, the MR and GR were purely associated with a genomic role as they act as transcription factors within the nucleus (de Kloet et al., 2005; Datson et al., 2008). While this is generally true, corticosteroids can also influence a wide range of behaviors and endocrine outputs within minutes, a time frame that is too rapid to be explained by genomic effects (Groeneweg et al., 2011). In agreement, we and others recently established that corticosteroids rapidly alter neuronal activity and excitability in a number of brain areas (Di et al., 2003; Karst et al., 2005, 2010; Tasker et al., 2006). Several of these rapid actions require the MR (and some also the GR) and seem to occur by corticosteroids binding to a molecule that is accessible from the outside of the cell membrane. In agreement, a subpopulation of the MR and GR have been shown to be present at the plasma membrane (Johnson et al., 2005; Prager et al., 2010). Despite considerable knowledge regarding the functional significance of membrane-initiated corticosteroid signaling, the molecular pathways underlying these actions are just beginning to be unraveled in neurons (see also *Chapter 2*).

In vitro cell lines have been very valuable to examine the effects of aldosterone or corticosterone through the MR on cell signaling. The identification of many signaling partners of membrane-associated MR signaling has been accomplished in cell lines, including cAMP, ERK1/2, G-proteins, caveolin-1, PKC and PI3K (Grossmann and Gekle, 2009; Dooley et al., 2012). Additionally, structure-function relationships can be delineated. Thus far, it has been established that transfection of the ligand binding domain of the MR is sufficient for aldosterone to rapidly activate the ERK1/2 pathway (Grossmann et al., 2008). For other steroid receptors mutations of single amino acids have aided the understanding of the membrane translocation pathways of these receptors (Levin, 2009). However, the genomic actions of corticosteroids are greatly affected by cell-context (John et al., 2011) and remarkably low overlap in corticosteroid regulated gene patterns were found between neuronal and non-neuronal cells types (Polman et al., 2012, 2013). Whether non-genomic corticosteroid actions are also different between neuronal and non-neuronal settings remains to be addressed. In addition, numerous single nucleotide polymorphisms (SNPs) in the MR gene, including the promoter region, have found to be associated with variability in neuroendocrine and autonomic activity (Martinez et al., 2009; DeRijk et al., 2011; van Leeuwen et al., 2010a,b) and the occurrence of psychiatric symptoms (Kuningas et al., 2007; Klok et al., 2011). Functional *in vitro* models would be valuable to investigate whether altered brain function associated with MR SNPs is purely explained by MRs genomic actions and expression levels or whether they also depend on the non-genomic membrane-associated functions of the MR.

Earlier, potassium currents of hippocampal cells were reported to be rapidly affected by MRs. The amplitude of fast-inactivating (A-type) potassium currents in CA1 neurons reduced rapidly after corticosterone application (Olijslagers et al.,

2008). This effect was prevented by pretreatment with an MR antagonist. A-type channels are important for determining firing frequencies and to reduce the amplitude of back-propagating action potentials in dendrites (Hoffman et al., 1997). As such they are important for plasticity and excitability. For example, deletion of A-type channels potentiates the induction of LTP (Chen et al., 2006). A decrease in A-type current amplitude after corticosterone application would thus enhance plasticity and excitability in neurons.

Potassium currents can be induced in multiple neuronal-like cell lines. The widely used PC12 cell line expresses multiple types of voltage-dependent potassium channels (Hoshi and Aldrich, 1988; Castillo et al., 2001), including fast-inactivating A-type currents. In addition, a number of neuroblastoma cell lines show expression of multiple subtypes of potassium and other ion channels. Of these, the mouse neuroblastoma cell line N1E-115 shows induction of large amplitude potassium currents with both inactivating and non-inactivating components (Hirsh and Quandt, 1996; Lima et al., 2008).

Here, we tested the feasibility of using *in vitro* neuronal-like cell lines to mimic non-genomic effects of corticosterone on potassium currents, with the ultimate aim of unraveling the underlying mechanism. As both these cell lines are devoid of endogenous MR, we can further test whether MR expression is sufficient for rapid corticosterone actions to occur.

3.2 Methods

Compounds

Corticosterone was obtained from Sigma and first diluted in EtOH to a concentration of 15 mM and next to the final concentration in PBS or recording medium. The same concentration of EtOH was used as vehicle. Corticosterone-BSA (cort-BSA) was dissolved to a concentration of 12.5 µM in 0.9 % NaCl, 0.25 % carboxymethyl cellulose and 0.2 % Tween (solvent A). There are 23 molecules of corticosterone bound to one BSA-molecule, therefore 4.4 nM cort-BSA matches 100 nM of free corticosterone.

Cell culturing procedures and plasmids

In addition to PC12-Neurocreen-1 (NS-1) and N1E-115 cells, in some experiments COS-1 or CHO cells were used. COS-1 cells are maintained in high glucose DMEM and CHO cells in F-12 medium (both GIBCO), both supplemented with 10 % fetal bovine serum (FBS) and 1 % penicillin and streptomycin. The pRSV-MR plasmid that was used contains the human MR gene under a Lac promotor (kind gift of R. Evans (The Salk Institute for Biological Studies, La Jolla, CA)). pEYFP-hMR was generated by cloning the MR gene from the pRSV plasmid into the pEYFP-C1 plasmid (described in more detail in *Chapter 6*), generating an N-terminally YFP-tagged MR. pEYFP-C1 was from Addgene.

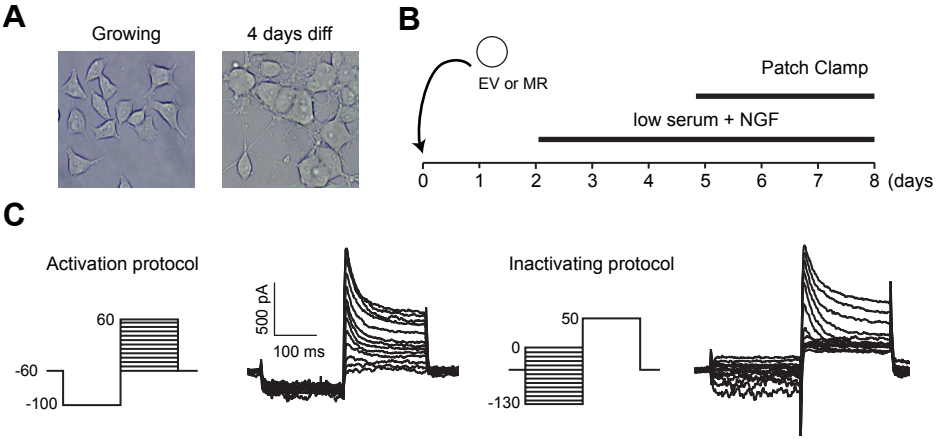

Figure 3.1: Patch protocols for NS-1 cells
(A) 3 days of NGF application leads to a neuronal-like phenotype in NS-1 cells. (B) The general experimental outline of single-cell patch clamp experiments in NS-1 cells. (C) Voltage dependency of the potassium currents are obtained with the activation (left) and inactivation protocols (right). Example currents are shown next to the corresponding protocols.

NS-1 cells

NS-1 cells were maintained in RMPI 1640, supplemented with 10 % horse serum (HS), 5 % FBS and 1 % penicillin and streptomycin. Throughout culturing, all plates and coverslips were pre-coated with collagen (60 µg / 10 cm^2, overnight at RT) to enable better cell attachment. DNA transfection was performed with an electroporation method, using the Amaxa Nucleofection apparatus (Lonza). In short, NS-1 cells were trypsinated and divided in 1 mln aliquots and spun down. Cell pellets were dissolved in 100 µl prewarmed nucleofector-solution, carefully mixed with 5 µg DNA and transferred to a certified cuvette for electroporation (program U29). Immediately after, cells were remixed with growth medium and plated onto collagen coated ø 13 mm coverslips, allowing differentiation 24 h later. For NS-1 cells, differentiation into a neuronal-like phenotype is acquired with a combination of serum starvation and nerve growth factor (NGF) treatment. At 24 h after transfection, culture medium was replaced for low serum medium (RMPI 1640 supplemented with 3.4 % HS and 1.6 % FBS). After 24 h this was replaced for fresh low serum medium with 0.05 % NGF. Cells were kept in NGF-containing low serum medium for 3–5 days and medium was replaced every 2 days. NS-1 cells can differentiate into an adrenocortical-like phenotype with glucocorticoids, therefore all sera used in the low serum medium were 2× charcoal-stripped to bind and wash away all reminiscent endogenous hormones. Cells were used for electrophysiology after 3–5 days of NGF treatment (the timeline of all procedures is summarized in Figure 3.1B).

N1E-115 cells

N1E-115 cells were maintained in low glucose DMEM, supplemented with 10 % FBS and 1 % penicillin and streptomycin. N1E-115 cells differentiate into a neuronal-like cell type with serum starvation and 2 % DMSO. Thus, cells were plated onto ø 13 mm coverslips coated with poly-l-lysin (100 µg/10 cm^2, 2 h at RT). 24 h after plating, normal growth medium was replaced for differentiation medium (low glucose DMEM, supplemented with 2 % FBS and

2 % sterile DMSO; medium replaced every 2 days). N1E-115 cells were transfected with lipofectamine (Life Technologies) during differentiation. In short, cells were washed with PBS and transfected in empty DMEM according to normal protocol (lipofectamine:DNA = 3:1, 1 µg DNA / 100 000 cells). Cells were incubated with the lipofectamine-DNA mixture for 4 h and thereafter replenished with differentiation medium. Cells were used for electrophysiology 2–3 days after transfection, thus after 6–7 days of differentiation (for the time line see Figure 3.6B). 24 h before patch clamping, normal differentiation medium was replaced for media containing charcoal-stripped sera to prevent effects of endogenous hormones.

Western blot

For Western blot analysis of MR and control proteins, cells were transfected with the required plasmids, harvested 48 h after transfection and prepared for western blot. Protein lysates, SDS-polyacrylamide gel electrophoresis and Western blotting were performed as described previously (Vreugdenhil et al., 2007). For each experiment, equivalent amount of samples (10–15 µg) were used. The blots were incubated with 1:500–2500 MR 1D5 or 2B7 antibodies (both are generous gifts of Gomez-Sanchez (Gomez-Sanchez et al., 2006)) and co-assessed for α-tubulin (1:5000; Sigma-Aldrich) in combination with 1:5000 goat-anti-mouse IgG HRP. All antibodies were diluted in TBST with 0.5 % milk powder. Primary antibody incubation was done for 1 hour at RT or for 16 hours at 4 °C. Detection was performed with the ECL detection system (GE Healthcare).

Immonufluorescence staining

For immunofluorescence stainings cells were plated on collagen-coated coverslips (diameter 12 mm) and used for experiments 48 h after transfection. If required, cells were treated with hormones or vehicle for 2 h before fixation. Fixation was performed with 4 % paraformaldehyde (PFA) for 30 min at RT. Subsequently, cells were permeabilized with 0.5 % Triton-100 in PBS, incubated with primary antibody (1:1000 MR 1D5 antibody (Gomez-Sanchez et al., 2006)) in PBST (0.1 % Triton-100 in PBS), supplemented with 1 % BSA for 60 min. Next, cells were incubated for 60 min with 1:1000 goat-anti-mouse AlaxaFluor488 (or 594) in PBST with 1 % BSA and finally for 10 min with 1:5000 with Hoechst 33342 (Life Technologies) for nuclear counterstaining (all in the dark). Between all steps, cells were washed for 3×5 min with PBST. Cells were mounted with Aqua Poly/Mount (Polysciences) and imaged on a conventional fluorescence microscope (Leica DM6000). For YFP-MR, fixation, permeabilization and Hoechst staining and mounting were performed according to the same protocol, but no antibodies were applied.

qPCR

For RT-qPCR, NS-1, N1E-115 and COS-1 cells were either left untransfected or transfected with 5 µg EV, 1, 5, or 10 µg MR / mln cells (with their respective transfection methods) and harvested by TRIZol method 48 h later. Reminiscent DNA was removed by DNAse treatment (Life Technologies, 1 µl DNAse for 1 µg DNA). Subsequently, cDNA was synthesized using the iScript kit (Bio-Rad). A set of 20 bp primers was designed to span a 220 bp region in exon 2–3 of the MR. RT-qPCR was conducted using the capillary-based LightCycler® thermocycler and fast start DNA masterPLUS SYBR Green I kit (Roche) according to the manufacturers'

instructions and described in more detail in (Polman et al., 2012). All samples were run twice and relative expression levels were calculated with a generated standard curve.

Luciferase essay

For the luciferase essay, cells were transfected with a combination of 500 ng/10 cm^2 YFP, YFP-MR or MR together with 100 ng/10 cm^2 TAT3-Luciferase (tyrosine amino transferase triple hormone response element) and 2 ng/10 cm^2 pCMV-Renilla (Promega). 24 h after transfection cells were treated with 10 nM corticosterone, 10 nM aldosterone or 0.001 % EtOH in culture medium supplemented with charcoal stripped FBS. After 20 h, cells were lysed with passive lysis buffer and firefly and renilla luciferase luminescence was determined according to the general prescription of the dual label reporter essay (Promega) on a luminometer (CENTRO XS3 LB960, Berthold). For analysis, the ratio of the two luminescent signals were used to control for differences in transfection efficiency and cell density.

Electrophysiology

Differentiated NS-1 or N1E-115 cells plated on ø 13 mm coverslips were submerged in recording solution in a custom made recording chamber. For NS-1, recording medium contained 130 mM NaCl, 5 mM KCl, 2 mM $CaCl_2$, 1 mM $MgCl_2$, 10 mM HEPES and 5 mM glucose, supplemented with 10 mM tetraethylammonium (TEA) to block sustained potassium currents, pH 7.3 adjusted with NaOH (all from Sigma-Aldrich). For N1E-115 cells, no TEA was added and molarity was compensated by using 15 mM glucose. Throughout the recordings the recording solution was continuously refreshed and kept at 32 °C. For both cell lines, the recording pipette contained: 140 mM KCl, 10 mM HEPES, 5 mM EGTA, 2 mM $MgCl_2$, 0.1 mM $CaCl_2$, 2 mM MgATP and 0.4 mM Na_2GTP (pH 7.3 adjusted with KOH; all from Sigma-Aldrich). Cells were imaged with an upright microscope (Axioskop 2 FS plus, Zeiss), equipped with differential interference contrast and wide field fluorescence. Healthy and well differentiated cells were identified manually and patched using 4–6 MΩ borosilicate glass electrodes (0.86/1.5 mm inner/outer diameter, Harvard Apparatus). For some experiments, GFP or YFP-MR fluorescence was checked with wide field fluorescence and moderately fluorescent cells were chosen for patch clamping. To prevent phototoxicity, fluorescence exposure duration was kept at a minimum and low intensity fluorescence was used. Whole cell voltage clamp recordings were made with an Axopath 200B amplifier (Axon instruments) interfaced to a computer via a Digidata (type 1322A; Axon Instruments). After reaching a gigaseal, the membrane patch was ruptured and the cell was kept at a holding potential of −60 mV (NS-1) or −70 mV (N1E-115). Series resistance was compensated for 60 %. To test voltage dependency of A-type current activation and inactivation, two types of protocols were used. Protocol 1 tested activation properties by changing the activation step from −60 mV to +60 mV in 10 mV steps. Protocol 2 tested voltage dependency of inactivation by changing a prepulse from 0 mV to −130 mV in 10 mV steps. Duration of the voltage steps differed for NS-1 and N1E-115 cells, all protocols are shows in Figure 3.1C and 3.6C.

Data analysis was performed with ClampFit (Molecular Devices). Data was corrected for leak current and baseline and maximum current amplitudes were recorded and plotted against voltage steps. Half maximal values were calculated as the first voltage step where the half maximum amplitude was achieved.

Statistics and data representation

Rapid effects of compounds on potassium currents were tested with two-tailed paired samples t-tests on the original, uncorrected data. Due to large differences in basal amplitudes between cells, the A-type current data is represented as % of maximum amplitude during baseline recordings in all figures. All between-subject comparisons were performed with two-tailed independent sample T-tests for comparisons of 2 groups or one-way ANOVAs for < 2 groups.

3.3 Results

A-type currents in Neuroscreen-1 cells

PC12 cells are a well-known neuronal-like cell line that shows large potassium currents upon differentiation (Hoshi and Aldrich, 1988; Castillo et al., 2001). Neuroscreen-1 (NS-1 cells are a subclone of PC12 cells with a higher responsiveness to NGF (Dijkmans et al., 2008). Upon stimulation with NGF, NS-1 cells show neuritogenesis within a day and develop a network of extensive neurites within 2–5 days upon NGF-induced differentiation (Dijkmans et al., 2008). We recorded single well-differentiated NS-1 cells in the voltage-clamp mode after 3–5 days of differentiation. Comparable to their parent strain, differentiated NS-1 cells showed large potassium currents with a large non-inactivating (delayed rectifier) and a smaller fast-inactivating (A-type) component. The delayed rectifying component was effectively blocked by $10\,\text{mM}$ TEA, thus revealing clear rapidly inactivating A-type currents (Figure 3.1C). The maximum A-type current amplitude (at $+60\,\text{mV}$) showed large cell-to-cell variation, ranging from 145 to $5600\,\text{pA}$, with an average of $1491 \pm 155\,\text{pA}$ ($n = 59$). A-type currents are most efficiently activated with a hyperpolarizing prepulse preceding the depolarizing step, relieving the voltage-dependent inactivation of the channels. Indeed, we found that a prepulse of $-130\,\text{mV}$ increases the potassium current to a subsequent depolarization by 2.5 ± 0.4 fold (compared to stepping directly from a holding potential of $-60\,\text{mV}$). NS-1 A-type currents were half maximally activated with a depolarization to $20.2 \pm 1.3\,\text{mV}$ and the half maximal value for inactivation was $-71.6 \pm 2.8\,\text{mV}$. Further characterization of the currents is presented in Figures 3.1 and 3.2.

Corticosterone and cort-BSA reduce A-current amplitude only after MR transfection

In the mouse hippocampus, corticosterone application led to a reduction in A-type current amplitude and a shift in activation properties so that larger depolarizations were required for the induction of similar A-type currents (Olijslagers et al., 2008). These effects were shown to require the MR. PC12 cells do not express endogenous MR (Lai et al., 2005).

First, we tested whether corticosterone could similarly affect A-type current amplitudes in NS-1 cells transfected with an empty vector (EV). In EV-transfected NS-1 cells, we observed a small, but statistically significant, decrease in maximal A-type current amplitudes (-12.4 ± 0.5 % compared to baseline; Figure 3.2A,B), presumably due to run down of cells during the patch procedure.

Next, we electroporated NS-1 cells with a plasmid containing human MR and induced differentiation the next day. The transfection efficiency of this method was assessed with transfection with (untagged) GFP. We found that the transfection efficiency was very high: 24 h and 48 h after transfection 89.4 ± 1.1 % and 90.1 ± 1.4 % of cells respectively was GFP positive ($n = 12$ wells). Due to differentiation cells do not divide and transfection efficiency is thus not expected to drop significantly over time, although this was not verified directly. We observed a rapid action of corticosterone on A-type currents in MR transfected cells. Within 5 to 10 minutes after application of 100 nM corticosterone, A-type current amplitudes were strongly reduced (Figure 3.2A and C, top panel). This effect was most apparent with high depolarization steps. No effect was seen on activation or inactivation properties. Thus, the maximum A-type current amplitude was reduced to 64.7 ± 0.1 % of baseline levels, but the voltage dependency of the channels was unaffected (Figure 3.2C–E, ½ max of 15.7 ± 2.2 mV). This reduction of maximal A-type current amplitudes was significantly greater than in EV-transfected cells. In its non-genomic role, corticosterone has been reliably show to act at the cell membrane (Groeneweg et al., 2012). We therefore tested the effect of BSA-conjugated corticosterone (cort-BSA), a membrane-impermeable conjugate of corticosterone. Comparable to corticosterone, also cort-BSA application led to a reduction of the maximal A-type current amplitude (to 72.6 ± 6.2 % of baseline levels), but did not affect voltage dependencies of the channels (Figure 3.2C, middle panel). Finally, vehicle treatment led to a much smaller reduction of A-type amplitudes in MR-transfected NS-1 cells (to 84.6 ± 4.4 % of baseline levels, Figure 3.2C, bottom panel).

To conclude, we show that we can reproduce —in cell lines *in vitro*— the rapid, membrane-initiated reduction of A-type current amplitudes earlier observed in hippocampus slices. Moreover, here we show that expression of the MR is not only required for these effects, but MR expression is sufficient to obtain non-genomic corticosterone-induced effects.

Instability of MR protein in NS-1 cells leads to failure to reproduce results

We transfected NS-1 cells with a method known to give high transfection efficiency and with an MR plasmid (pRSV-MR) known to induce robust MR protein expression in other cell lines (Klok et al., 2011). However, when we assessed MR expression by Western blot 48 h after electroporation we failed to find any MR protein (Figure 3.3A). As a control we also transfected COS-1 cells with the same pRSV-MR plasmid and here we found a clear MR positive band of the expected size (107 kDa)

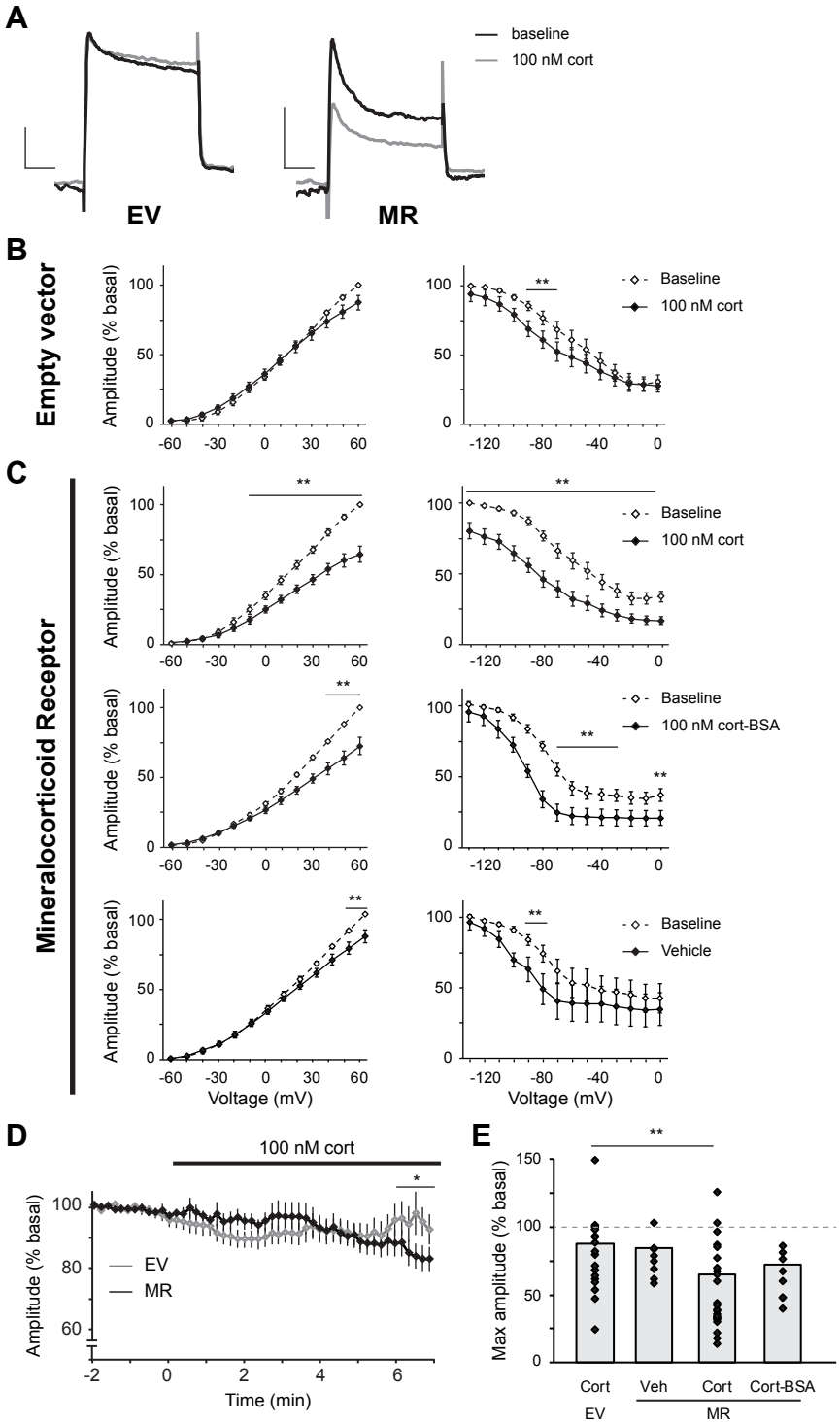
A
baseline
100 nM cort
EV
MR
B
Empty vector
Amplitude (% basal)
Baseline
100 nM cort
C
Mineralocorticoid Receptor
100 nM cort-BSA
Vehicle
Voltage (mV)
D
100 nM cort
EV
MR
Time (min)
E
Max amplitude (% basal)
Cort
Veh
Cort
Cort-BSA
EV
MR

in transfected cells. Similarly, prolonged exposure, different transfection procedures or a different MR antibody (N2B7 (Gomez-Sanchez et al., 2006)) all failed to show MR expression in transfected NS-1 cells (data not shown). The MR is known to be a very unstable protein and can be lysed during lysate preparations leading to fragments of incorrect size (Gomez-Sanchez et al., 2011). However, even though we did observe fragments of incorrect size on the Western blot (Figure 3.3A), these were seen in both transfected and untransfected NS-1 cells and are likely to be due to aspecific interactions of the antibody.

Next we initiated a number of different biochemical approaches to test for presence of MR protein. First, we showed that MR immunofluorescence is indistinguishable between NS-1 cells transfected (according to normal procedure) with the MR or EV with immunofluorescence staining (Figure 3.3B). Again, COS-1 cells transfected with MR showed clear MR immunofluorescence and in the expected pattern of enhanced nuclear localization. Secondly, we obtained YFP-tagged MR and assessed YFP fluorescence in YFP-MR transfected NS-1 cells after treatment with vehicle or 100 nM corticosterone for 2 h. Also here, we failed to find a higher fluorescence in transfected cells compared to untransfected cells (Figure 3.3C); neither was there an indication of nuclear translocation of the YFP signal to the nucleus (data not shown). Transfection of YFP or GFP alone did lead to clear fluorescence throughout the cell (Figure 3.3C). As a final attempt, we assessed MR function with a transactivation essay. We cotransfected NS-1 or COS-1 cells with MR, EV or YFP-MR with Firefly luciferase under an MR-dependent TAT3 promotor (van Leeuwen et al., 2010a; Klok et al., 2011), and Renilla luciferase under a control (CMV) promotor. In COS-1 cells, we observed an increase in Firefly-to-Renilla luminescence ratio after transfection with either the MR or YFP-MR (Figure 3.3D). As expected, treatment with either corticosterone or aldosterone (10 nM for 16 h) resulted in a 6 and 7 fold increased Firefly luciferase production respectively. In contrast, in NS-1 cells there was no increase in Firefly-luciferase induction in MR or YFP-MR transfected cells. We did

Figure 3.2 *(preceding page)*: A-type currents are reduced by corticosterone only in MR-expressing NS-1 cells
(A) Example of A-type currents from NS-1 cells transfected with an empty vector (EV) (left panel) or the MR (right panel). Corticosterone induces a reduction in A-type current amplitude for MR-transfected, but not for EV-transfected NS-1 cells. Currents elicited with -100 mV priming and 60 mV depolarization step, scale bars: 500 pA (vertical) and 50 ms (horizontal). (B-C) A-type currents are measured before and 10 to 15 minutes after hormone treatment with the activation (left) and inactivation (right) protocols. (B) In NS-1 cells transfected with an empty vector (EV), corticosterone only marginally affects the amplitude of A-type currents. (C) NS-1 cells transfected with pRSV-MR. In MR-expressing cells, both 100 nM corticosterone (top) and 100 nM cort-BSA (middle) treatment results in decreased A-type current amplitudes. Vehicle treatment has little effect (bottom). (D) The effect of corticosterone on A-type current amplitude is rapid in onset, as a significantly reduced current amplitude is already observed after 6 minutes. No significant reduction is observed for EV-transfected cells. (E) The decrease in maximum A-type current amplitude ($+60$ mV step) is significantly larger in the MR-cort versus the EV-cort group. *Statistics. (A-C) Paired samples t-test. Significant effects with $p < 0.01$ are shown. (D) Repeated measures (against baseline). (E) One-way ANOVA with post hoc multiple comparison (Tukey). Group sizes: EV+cort $n = 20$, MR+veh $n = 8$, MR+cort $n = 23$, MR+cort-BSA $n = 8$ (cells).* $** = p < 0.01$.

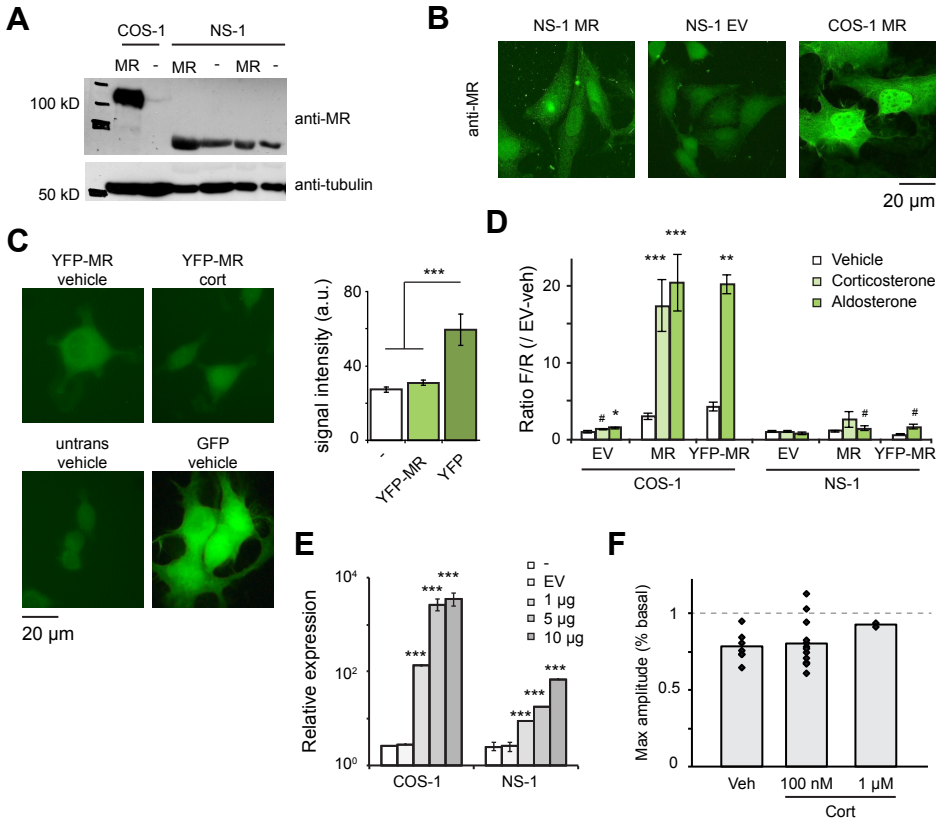

Figure 3.3: MR mRNA is present, but MR protein absent from MR-transfected NS-1 cells
NS-1 cells do not show detectable MR protein expression after pRSV-MR transfection in NS-1 cells. (A-D) (A) Representative western blot of MR expression after MR transfection in COS-1 and NS-1 cells. There is no appreciable MR protein expression 48 h after transfection in NS-1 cells, while MR protein is clearly seen in transfected COS-1 cells. Expected size of MR: 107 kDa. α-tubulin is coassessed as loading control. (B) Representative IF images for MR do not show quantitative difference in fluorescence between MR and EV-transfected NS-1 cells. In COS-1 cells, clear MR IF signal is seen with, as expected a high nuclear localization. (C) Transfection with YFP-MR does not lead to detectable YFP fluorescence 48 h after transfection, nor is there an accumulation of fluorescence in the nucleus after corticosterone treatment. Transfection of YFP alone does show clear YFP fluorescence in NS-1 cells. Quantification of average IF levels is shown on the right. (D) Transactivation essay. COS-1 and NS-1 cells are transfected with MR, YFP-MR or EV and the ratio between MR-driven Firefly and control-driven Renilla luminescence is assessed 48 h after transfections. In COS-1 cells, both aldosterone and corticosterone (10 nM, 16 h) induce an increased Firefly/Renilla ratio. In NS-1 cells, however, corticosterone does not affect the Firefly/Renilla ratio and aldosterone does so only marginally. (E) MR mRNA levels assessed with RT-qPCR. In contrast to the lack of detectable MR protein and function, there is clear MR mRNA expression 48 h after pRSV-MR transfection in NS-1 cells, albeit in a > 100 fold lower amount as in COS-1 cells. (F) The corticosterone-induced decrease in A-type current amplitude is not reproduced in a new set of MR-transfected NS-1 cells. Both 100 nM and 1 µM corticosterone fail to induce a decrease of maximum A-type current amplitude ($n = 13/2$). *Statistics. Independent-samples t-test against untransfected condition in C and E and against corresponding vehicle conditions in D.* $\# = p < 0.1, * = p < 0.05, ** = p < 0.01, *** = p < 0.001$

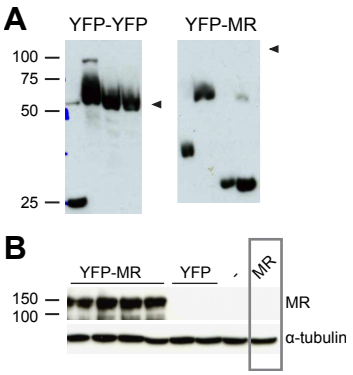

Figure 3.4: Stable MR cell lines show selection against MR expression
(A) Clones of CHO cells stably transfected with YFP-YFP (52 kDa; left panel) or YFP-MR (137 kDa; right panel) and stained for YFP (1:1000). For YFP-YFP clones, 3 out of 4 show a primary band at the expected size. However, none of the 4 putative YFP-MR clones show a band at the correct size (indicated by triangle), but instead a selection of low weight protein bands suggestive of YFP with a small portion of the MR attached. (B) Western blot for an assortment of CHO cells. Band to the right is of clone A09 previously described to be stably expressing the MR (Grossmann et al., 2005). No MR band is seen for this sample, while clear bands are seen in cells transiently transfected with YFP-MR (left). MR: 1D5 antibody 1:1000.

observe a small, but statistically significant, increase in Firefly-to-Renilla ratio after aldosterone treatment, i.e. 1.4 to 2.4 fold in MR and YFP-MR transfected cells respectively which was not seen in EV-transfected cells (Figure 3.3D). Possibly, this indicates a very low expression of the MR.

A failure to induce MR protein expression after transfection could be due to a low transfection efficiency or due to autolysis of the expressed protein within the cells. We showed clear expression of GFP and YFP (both under a CMV promotor) after electroporation in NS-1 cells, but failed to find expression of pRSV-MR (Lac promotor) or YFP-MR (CMV promotor), thus it is unlikely that the lack of protein expression was due to problems with transfection efficiency or transcription of the transfected plasmids. Still, to verify that MR DNA was expressed and transcribed in transfected NS-1 cells, we measured MR mRNA levels. As shown in Figure 3.3E, we found clear expression of MR mRNA in both COS-1 and NS-1 cells after transfection with increasing levels of the MR plasmid. Thus, transfection with 1 µg, 5 µg and 10 µg (/mln cells) MR resulted in 4-, 8- and 15-fold higher mRNA levels respectively. MR mRNA levels in NS-1 cells were > 100 fold lower than what is seen in COS-1 cells after transfection with similar doses of MR plasmid (Figure 3.3E). Also in differentiated cells, 7 days after transfection, there was still clear MR mRNA expression, although this was approximately 4-fold lower compared to that found 48 h after transfection (data not shown).

In an additional set of experiments, we attempted to create stable expression of YFP-tagged MR in CHO cells. However, while the procedure led to successful expression of another YFP construct (YFP-YFP) in 3 out of 4 clones, for YFP-MR all YFP positive clones only had fragments of the MR attached (Figure 3.4A). Similarly, the group of Claudia Grossmann and Michael Gekle had successfully created stable expression of the MR plasmid in CHO cells (Krug et al., 2002; Grossmann et al., 2005). However, they observed decreasing levels of MR within these cells even under antibiotic selection and correspondingly, we found no indication of MR protein expression within these cells by Western blot (Figure 3.4B; personal communication with C. Grossmann).

In the first set of electrophysiological experiments we observed a reduction in potassium A-type currents specifically after MR transfection (Figure 3.2). This seems irreconcilable with the lack of MR protein expression observed. However, there was large variation between cells and no decrease in amplitudes was observed in about 25 % of cells (Figure 3.2E). Moreover, a new experiment where we electrophysiologically measured the effect of either vehicle, 100 nM corticosterone or 1 μM corticosterone in a new group of MR-transfected NS-1 cells failed to reproduce these earlier obtained results (Figure 3.3F).

Taken together, the MR protein seems to be highly instable in NS-1 cells. MR mRNA was observed after transfection of NS-1 cells with an MR plasmid. But, whereas the same plasmids resulted in clear and reproducible MR protein expression in COS-1 cells, we found no indications for MR protein expression after successful transfection in NS-1 cells. The MR is thus either not translated or immediately degraded in NS-1 cells, for reasons unknown to us. We have noted problems with MR expression on other occasions as well. Consequently, these expression issues make the NS-1 cell line unsuitable for reliable and reproducible electrophysiological experiments.

Potent MR protein expression in a second neuronal-like cell line: N1E-115 cells

A number of neuroblastoma-generated cell lines also show large potassium currents. Of these, the N1E-115 cells, a mouse neuroblastoma cell line, is known to express large amplitude potassium currents, consisting of a (slow-) inactivating and a non-inactivating component (Hirsh and Quandt, 1996; Lima et al., 2008; Vicente et al., 2010). It is unclear whether the inhibitory effect of corticosterone on fast-inactivating potassium currents seen in CA1 hippocampal cells (Olijslagers et al., 2008) is specific for a subtype of potassium channels or a more broad effect on (inactivating) potassium channels. Thus, we tested the effect of corticosterone on potassium currents in N1E-115 cells after transfection with MR.

We first employed a number of biochemical approaches to verify that MR protein was expressed and functional after transfection in N1E-115 cells. Indeed, on Western blots we found proteins of the correct size 48 h after transfection (Figure 3.5A). In addition, YFP-MR transfection showed clear YFP fluorescence in N1E-115 cells and nuclear translocation of YFP-MR after corticosterone treatment as expected (Figure 3.5B). Moreover, all MR plasmids (pRSV-MR, pcDNA3-MR and YFP-MR) led to the expression of a functional MR protein as shown by robust transactivational capacity (Figure 3.5C). Without additional hormone treatment, TAT3-Firefly luciferase was already produced at higher levels as compared to EV transfected cells. Treatment with 10 nM corticosterone for 16 h led to a strong induction of Firefly production when cotransfected with any of the three MR plasmids. The pRSV-MR plasmid (which was used in NS-1 cells) showed the lowest, but still apparent, transactivational capacity (Figure 3.5C). Finally, we also found clear MR

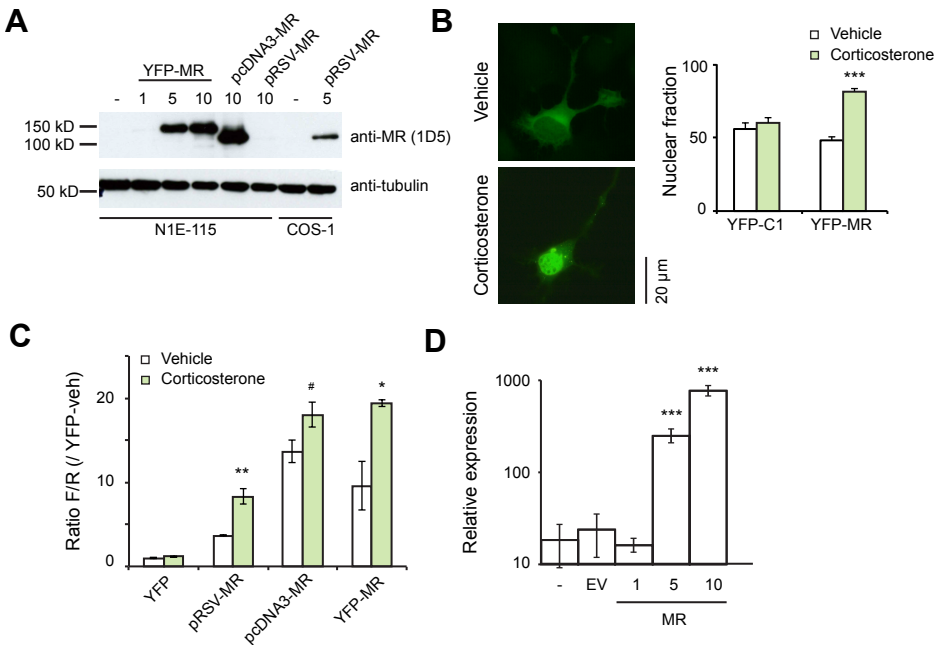

Figure 3.5: YFP-MR is robustly expressed in N1E-115 neuroblastoma cells
(A) Representative western blot assessed for MR. Transfection of increasing amounts of YFP-MR shows robust expression of YFP-MR protein (125 kDa). Similarly transfection with two different MR constructs results in expression of MR protein (107 kDa), with low levels after pRSV-MR transfection. α-tubulin is coassessed as loading control. (B) IF imaging shows clear YFP-MR fluorescence in transfected N1E-115 cells and nuclear translocation after corticosterone (10 nM, 4 h) treatment. (C) Transactivation essay. In MR-transfected N1E-115 cells the ratio between MR-driven Firefly and control-Renilla luminescence is increased as compared to EV-transfected cells. Additionally, the ratio is further increased after application of corticosterone (10 nM, 16 h) in cells transfected with MR plasmids and not with EV. (D) RT-qPCR on N1E-115 cells shows increasing amount of MR mRNA after transfection with 1, 5 and 10 µg of pRSV-MR. *Statistics. Independent-samples t-test against corresponding vehicle conditions in B and C and against untransfected condition in D.* $\# = p < 0.1, * = p < 0.05, ** = p < 0.01, *** = p < 0.001$

mRNA expression with increasing levels of MR transfection in N1E-115 cells 48 h after transfection (Figure 3.5D) and still detectable mRNA expression (2–3 fold lower compared to 48 h) after 5 days of differentiation (data not shown).

Corticosterone does not affect potassium currents in N1E-115 cells

Subsequently, we assessed if we obtained currents with the expected properties in differentiated N1E-115 cells. After 5 days of serum starvation and DMSO application we observed a neuronal-like phenotype in the cells with strong neuritogenesis (Figure 3.6A). We patch clamped N1E-115 cells after 4–6 days of differentiation and maintained the cells in voltage clamp mode to measure ion currents. Similar to what was reported before (Hirsh and Quandt, 1996; Lima et al., 2008), we found large outward currents, that showed both a slow-inactivating and a non-inactivating component (Figure 3.6C). Maximal amplitudes ranged from 820 to 7200 pA, with an average

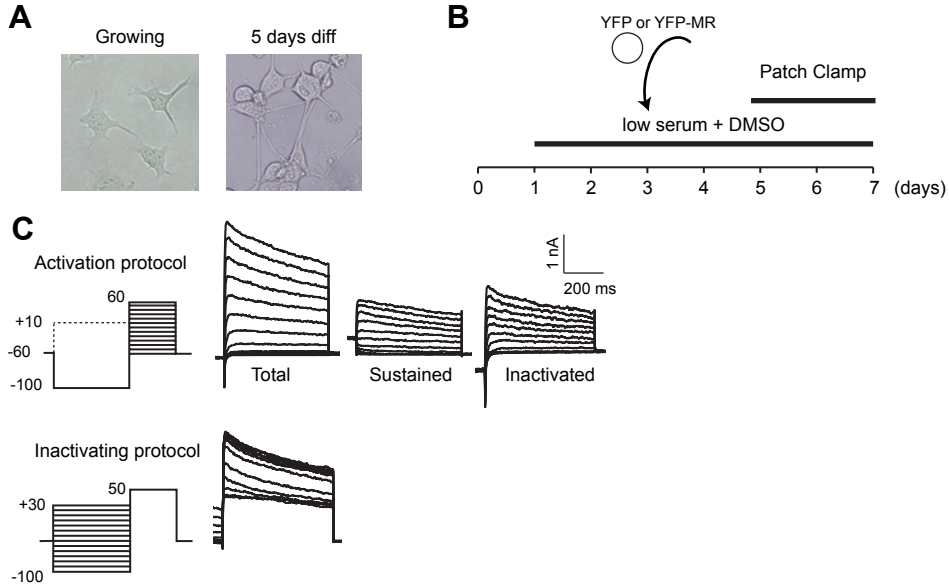

Figure 3.6: Patch protocols for N1E-115 cells
(A) N1E-115 cells develop a neuronal-like phenotype within 5 days of serum deprivation and DMSO treatment. (B) The general experimental outline of single-cell patch clamp experiments. (C) Voltage dependency of the potassium currents are obtained with the activation (top) and inactivation protocols (bottom). A combination of a sustained and an inactivating current is seen in N1E-115 cells. A prepulse of $+10$ mV generates only the sustained component, subtracting this from the total current generated the inactivating component. Typical traces are shown next to the corresponding protocols.

of 2366 ± 317 pA ($n = 19$). As expected (Lima et al., 2008), both current components were sensitive to TEA and 4-AP. Thus, at a dose of 1 mM, both TEA and 4-AP reduced the currents roughly by half, while an even stronger reduction was seen when both inhibitors were given simultaneously (Figure 3.7A). This is in sharp contrast to the A-type currents in NS-1 cells, which were recorded with 10 mM TEA in the recording medium. Finally, a hyperpolarized prepulse did not potentiate the potassium currents in N1E-115 cells. Thus, maximal potassium currents were already induced at resting potential, while the currents were partially inactivated by a preceding depolarization as expected (half maximum inactivation at -28.9 ± 3.8 mV, Figure 3.7B). In NS-1 cells hyperpolarizations did lead to larger A-type currents (½ max of -71.6 ± 2.8 mV). Finally, as compared to NS-1 cell A-type currents, in N1E-115 cells the voltage dependency of the currents was shifted marginally to the right (half maximal activation at $+23.7 \pm 3.8$ mV; Figure 3.7B). Thus, we found an overall potassium current in N1E-115 cells which is seemingly the combination of slow-inactivating and non-inactivating channels as was previously reported (Hirsh and Quandt, 1996; Lima et al., 2008).

We then chose to transfect YFP-MR instead of untagged MR to be absolutely sure that we only recorded from MR (protein) expressing cells. Thus, prior to patching we identified YFP-MR fluorescence and patched only fluorescent cells (we con-

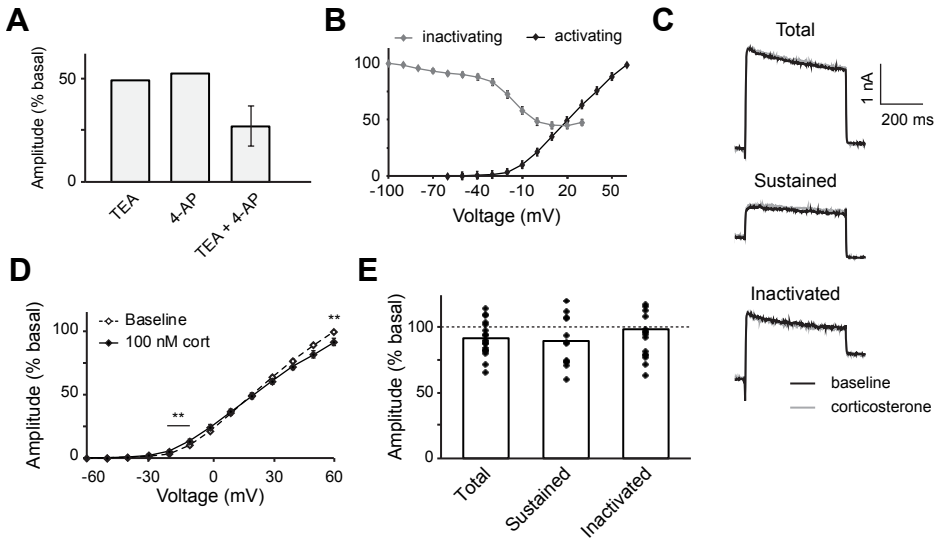

Figure 3.7: Potassium A-type currents show different kinetics in N1E-115 cells and are unresponsive to corticosterone
Differentiated N1E-115 cells are transfected with YFP-MR and YFP-expressing cells are identified and patched. (A) The potassium currents in N1E-115 cells are sensitive to both TEA (1 mM) and 4-AP (1 mM). The two compounds also have an additive effect. (B) The voltage dependency of the N1E-115 potassium currents is obtained with the activation and inactivation protocols. The potassium current in N1E-115 cells is not potentiated by a hyperpolarized prepulse. (C) Typical potassium currents elicited with a -100 mV prepulse (total), a $+10$ mV prepulse (sustained) and by subtracting the two (activated) shows in baseline and 5–10 min after 100 nM corticosterone (all $+60$ mV depolarization step). (D) Total potassium currents are assessed with the activation protocols before and 10–15 minutes after treatment with 100 nM corticosterone. Corticosterone does not affect the amplitude or voltage dependency of potassium currents in YFP-MR expressing N1E-115 cells ($n = 19$ cells). (E) Maximal amplitudes (at $+60$ mV) of either the total current, the sustained current or the inactivated current are only marginally lower than baseline values after corticosterone treatment. *Statistics. (D) Paired sample t-test ($n = 19$). Significance with $p < 0.01$ is shown.* $** = p < 0.01$

stricted ourselves to cells with moderate levels of YFP). As before, we measured the activating and inactivation characteristics of the potassium currents in baseline condition and within 5–10 minutes of corticosterone treatment; the results are presented in Figure 3.7C-E. The data shows that corticosterone application did not affect the overall potassium current in N1E-115 cells. Neither activation, nor inactivation voltage dependency were affected by corticosterone treatment. There was a marginal decrease in maximal amplitude (8.4 ± 3.0 %), but this was more indicative of some run down of the currents than of a corticosterone-specific effect. As the potassium current in N1E-115 cells is comprised of two components we also tested the effect of corticosterone treatment on each component separately. To do so, we inactivated the transient component with a depolarizing prepulse ($+10$ mV) and thus obtained only the sustained component. The inactivating component was then obtained by subtraction of the sustained components from the total current (Figure 3.6C). However, neither the sustained current nor the inactivated current

were affected by corticosterone treatment (maximal amplitudes of 89.7 ± 5.5 % and 98.2 ± 5.3 % of baseline levels respectively, Figure 3.7E).

3.4 Discussion

Rapid, non-genomic actions of corticosterone are increasingly accepted as functionally important action of corticosteroids. Within minutes after a stressful event or an otherwise achieved surge in corticosteroids a shift in neuronal excitability is induced in multiple brain areas (Karst et al., 2005, 2010; Tasker et al., 2006), potentially resulting in increased learning and behavioral reactivity (Khaksari et al., 2007; Groeneweg et al., 2011). The MR is required for many of these effects and involves a membrane-associated receptor, but the downstream signaling pathways and structure-function relationship remain ill understood.

We here sought to mimic a functional non-genomic action of corticosterone on neuronal excitability in a cell line, affording the possibility to alter the MR structure and signaling through transfection. Initially, in NS-1 cells we found the amplitude of rapidly-inactivating potassium currents to be strongly and significantly reduced by 100 nM corticosterone in a rapid, membrane-initiated and MR-dependent fashion (Figure 3.2). A lack of a corticosterone-induced effect in empty vector transfected NS-1 cells further suggests that the presence of the MR is sufficient to render (neuronal-like) cells responsive to non-genomic corticosterone actions. We did not observe the shift in voltage dependencies of the channels which was shown in CA1 neurons (Olijslagers et al., 2008). In N1E-115 cells, the sustained and slowly-inactivating potassium currents were not affected by corticosterone (Figure 3.7), suggesting that corticosterone only affects the kinetics of a specific subset of potassium channels.

Instability of the MR in cell lines

Much care must be taken in interpreting our current results as we were unable to reliably show the presence of the MR protein in MR-transfected NS-1 cells. Moreover, whereas we found a clear MR-specific effect of corticosterone in an initial large set of experiments ($n = 23$), we were unable to replicate these results in a further smaller subset of recordings ($n = 13$). We assessed potential MR protein expression by numerous methods, including Western blot, immunofluorescence staining, YFP-tagged MR transcripts and transactivation essays. Interestingly, while MR expression and functionality was found on all occasions in both COS-1 and N1E-115 cells, none of the methods showed expression in transfected NS-1 cells. Only aldosterone did show some transactivational potency in MR and YFP-MR transfected NS-1 cells, while this was absent in EV-transfected NS-1 cells. This finding could indicate a small, hard to detect presence of the MR in some of these cells.

The failure to detect a protein while mRNA is expressed could be caused by either an inhibition of mRNA translation or by protein degradation. Silencing of mRNA by microRNAs is recognized as an endogenous mechanism to inhibit translation (Lee et al., 1993; Bartel, 2004). The 3′ UTR region of the MR contains several microRNA recognition sites (de Kloet et al., 2009; Sõber et al., 2010) but their effect on MR expression has not been investigated. Moreover, the 3′ UTR region was not included in the plasmid DNA, making mRNA silencing through this route unlikely. As all steroid receptors, unliganded MR forms a multimer with several chaperones and heat shock proteins that keep it in its inactive conformation and that also protect against degradation (Yang and Fuller, 2012). Indeed, inhibition of HSP90, one of the main chaperones, leads to increased ubiquitylation and degradation of the MR (Faresse et al., 2010). Insufficient amounts of HSP90 might thus explain rapid degradation of transfected MR. However, HSP90 is endogenously expressed in PC12 cells. Moreover, steroid receptors share most, if not all, chaperones. To our knowledge there are no indications for an enhanced degradation of the MR and one study even found the opposite (Lightman et al., 2008). However, we and others have noted that the MR is a peculiar protein in *in vitro* settings. I will discuss the apparent instability of the MR *in vitro* in more detail in the general discussion (*Chapter 7*).

The lack of reliable MR protein expression is a likely explanation for the failure to reproduce the functional effects of corticosterone through the MR observed in the first series of experiments. We never assessed MR protein expression directly on cells that were also used for electrophysiology, thus, it remains possible that in this first series there was sufficient MR protein expression during recordings to induce the functional effects. Indeed, either mRNA silencing or efficient protein degradation are likely strongly affected by the cell context and could thus result in small fractions of viable MR protein depending on subtle differences in culturing conditions. Regardless, the lack of MR stability in NS-1 cells make this cell line unsuitable for further experiments.

Potassium channel subtypes and their responsiveness to corticosterone

While corticosterone —at least in the first series of recordings— affected the rapidly inactivating potassium currents in NS-1 cells, it had no effect on the potassium currents in N1E-115 cells. This suggests that the corticosterone-induced effects are specific for certain potassium channel subtypes. Potassium channels are the most diverse group of ion channels. Functionally, potassium currents can be grouped into transient or "A-type" channels and two subtypes of delayed rectifying channels; the slow-inactivating "D-type" and non-inactivating "M-type" channels. The potassium pore is formed by homo- or hetero-tetramers of α-subunits, encoded by one of the Kv families (Chandy et al., 1990; Vacher et al., 2008). Each type of current can be generated by a variety of channels. For example, A-type currents are generated by Kv1.4, Kv3.3, Kv3.4, Kv4.1, Kv4.2 or Kv4.3 channels (Vacher et al., 2008).

To build onto the complexity, heterotetramers form channels with intermediate kinetics and auxiliary (β) subunits affect the kinetics of the channels (Rettig et al., 1994). Neurons generally express multiple Kv subtypes, resulting in a summed cellular potassium current of intermediate kinetics. Olijslagers et al. (2008), found a reduction in A-type potassium currents by corticosterone in CA1 neurons. Within these neurons, A-type channels Kv1.4 and Kv4.2 are most abundantly expressed (Coetzee et al., 1999; Chen et al., 2006). The reduction in potassium amplitudes further required G-proteins and likely MAPK/ERK activation (Olijslagers et al., 2008). Kv4.2 is widely recognized as direct target of ERK1/2 (Schrader et al., 2006; Adams et al., 2008). ERK activation results in reduced surface expression, inhibition of current amplitude and a right-shift in activation kinetics of Kv4.2 (Yuan et al., 2002, 2006), making this subtype a prime candidate for corticosterone-induced regulation of potassium currents. However, ERK1/2 potentially affects other Kv subtypes as well (Yuan et al., 2006).

In PC12 cells, at least 4 different voltage-dependent potassium currents have been identified (Hoshi and Aldrich, 1988; Conforti and Millhorn, 2000). These include sustained, slow-inactivating and fast-inactivating currents. Of note, multiple studies reported transient A-type currents in only a small subset of differentiated PC12 cells (Hoshi and Aldrich, 1988; Conforti and Millhorn, 2000; Castillo et al., 2001), while others found them more frequently (Pannaccione et al., 2005, 2007). Although we did not quantify it here, we found clear A-type currents in the majority of NS-1 cells. It is possible that NS-1 cells represent a subclone of PC12 cells associated with larger (transient) potassium currents. Which Kv channels underlie the observed currents in PC12 cells remains a matter of debate; expression of many Kv subtypes, including the Kv1.2/1.3/1.4, Kv2.1, Kv3.1/3.2/3.3/3.4 and Kv4.2/4.3 channels, was found in PC12 cells (Conforti and Millhorn, 2000; McCrossan et al., 2003; Pannaccione et al., 2007). Highest expression of A-type channels was observed for the Kv3.4 and Kv4.2 channels. In NS-1 cells we recorded high amplitude A-type currents in the presence of 10 mM TEA. Whereas Kv3 channels are sensitive to TEA (Pannaccione et al., 2005), Kv4 subtypes are highly resistant (Coetzee et al., 1999). We thus presume that we recorded mainly from Kv4.2 mediated A-type channels. It thus seems likely that the reduction in A-type current amplitude found in CA1 neurons (Olijslagers et al., 2008) and here in NS-1 cells by corticosterone (albeit only in the first series) both involve actions on Kv4.2 channels. However, in CA1 neurons a decrease in maximal A-type current amplitude was seen in concert with a shift in the activation kinetics towards higher depolarizations (Olijslagers et al., 2008). In NS-1 cells we found no indications for a shift in kinetics. Whether this is due to different signaling cascades, different auxiliary subunits or a different Kv subunit composition remains to be established.

N1E-115 cells show two main potassium currents, a sustained current and a slowly-inactivating current (Quandt, 1988; Lima et al., 2008). Also for N1E-115 cells the channel subunits underlying the observed currents have not yet been deter-

mined in detail. One study, however, associated a reduction in Kv3.1 mRNA with a reduction in the slow-inactivating current (Hirsh and Quandt, 1996). Moreover, the inactivating current in N1E-115 cells is highly TEA sensitive, is not potentiated by a hyperpolarized prepulse and has slow inactivation kinetics, which all fit with Kv3.1 or Kv3.2 channels (Coetzee et al., 1999). Thus, we presume that the inactivating component of the N1E-115 potassium current is generated through a Kv3 channel (most likely Kv3.1) and this current is insensitive to corticosterone. Altogether, the data indicates that the suppressive effect of corticosterone on inactivating potassium currents is specific for some Kv channel subtypes and is not seen for slowly-inactivating Kv3.1 channels. Expression of specific Kv subtypes in isolation in non-neuronal cells could narrow down which Kv subtypes are responsive to rapid corticosterone actions.

In conclusion, the current experiments show that neuronal-like cell models can be used to reproduce a functional non-genomic effect of corticosterone on neuronal excitability. With the combination of NS-1 and N1E-115 cells we show that the reduction in potassium current amplitudes is Kv subtype specific. However, the stability of the MR in cell lines (at least the two we recorded from) is a limiting factor and must always be carefully monitored. Better understanding of MRs dynamics and half-life after transfection in cell lines would be very valuable to improve future models.